**MOTHER TERESA INSTITUTE OF SCIENCE & TECHNOLOGY**
**SATHUPALLY, KHAMMAM DIST., TELANGANA.**
**Institute RESEARCH & DEVELOPMENT**
**CELLAcademic Year: - 2022- 2023**

| S.No. | Date | Name of the Event | Purpose | Research Activity | Name of the Faculty |
|---|---|---|---|---|---|
| 1 | 02-09-2023 | RESEARCH & DEVELOPMENT CELL Committee meeting | Conformation of minutes of R&D Cell and Approvals | **Paper Publication:** High-Power Converter Based on the Wide Band Gap Power Semiconductor Devices for ElectricalDrive | Dr. Chlasani Hari Krishna |
| | | | | **Paper Publication:** Experimental chatter process stability using endmilling process on Al6061alloy with multiple bearing span conditions | Dr. Sk. Jakeer Hussain |
| | | | | **Paper Publication:** Investigation of the cutting-edge radius size effect on dynamic forces in micro end milling ofbrass260 | Dr. Sk. Jakeer Hussain |
| | | | | **NPTEL COURSE:** Principles of Management | Mr.M.Balaswamy |
| | | | | **NPTEL COURSE:** Quantum Mechanics-1 | Dr.M.V.Ramachandra Rao |
| | | | | **NPTEL COURSE:** Cloud Computing andDistributed Systems | Dr.Manjunath.BE |
| | | | | **NPTEL COURSE:** Cloud Computing andDistributed Systems | Mr.G.Ravi Raju |
| | | | | **NPTEL COURSE:** Data Base Management | Mr.G.Ravi Raju |
| | | | | **NPTEL COURSE:** Applied Linear Algebra inAI and ML | Mr.K S R K SUNIL |
| | | | | **NPTEL COURSE:** Introduction to EmbeddedSystem Design | Mr.Sk.Fhyasuddin |
| | | | | **NPTEL COURSE:** Air Pollution and Control | Mr.N.Vinod Kumar |
| | | | | **NPTEL COURSE:** Hydraulic Engineering | Mr.N.Vinod Kumar |

PRINCIPAL

*Journal of Harbin Engineering University*
*ISSN: 1006-7043*
Vol 44 No. 8
August 2023

# High-Power Converter Based on the WideBand Gap Power Semiconductor Devices for Electrical Drive

**C.Harinatha Reddy[1] , Y.V. Siva Reddy[2], Chalasani Hari Krishna[3], A. Pradeep Kumar Yadav[4],, T Brahmanada Reddy[5],N. Ravi Sankara Reddy[6]**

[1]Associate Professor in EEE Dept of G.Pulla Reddy Engineering College(Autonomous), Kurnool,
[2]Professor in EEE Dept of G.Pulla Reddy Engineering College(Autonomous), Kurnool.
[3]Associate Professor in EEE Dept, Mother Teresa Institute of Science and Technology, Khammam,
[4]Assistant Professor in EEE Dept, G.Pulla Reddy Engineering College(Autonomous), Kurnool,
[5]Professor in EEE Dept, G.Pulla Reddy Engineering College(Autonomous), Kurnool
[6]Associate Professor in EEE Dept of G.Pulla Reddy Engineering College(Autonomous), Kurnool,
[1]harinath.eee@gprec.ac.in,[2]yvsreddy.eee@gprec.ac,[3]chalasaniharikrishna@gmail.com,[4]pradeep.eee@gprec.ac.in[5]bramha.eee@gprec.ac.in,[6]ravishankar.eee@gprec.ac.in

**Abstract**—appropriate toward the objects restrictions, the conventional si- support control strategy move toward the fundamental restrictions of the matter within lots of behavior. The si- support procedure contain not be appropriate toward elevated electrical energy, elevated freq, elevated heat, elevated effectiveness plus elevated control compactness functions. appropriate toward the broad group space circuitry procedure encompass supreme electrical presentation of the si- support procedure, it be able to considerably decrease the burden of the inverter, amount, charge, plus augment effectiveness plus supremacy concentration influence electronic procedure, which be able to resist superior charge, earlier change rate, lesser button sufferers plus superior working connection warmth. The topic of elevated effectiveness, elevated supremacy compactness within the railing transfer electrical make insist since the conditions, the input expertise study of elevated influence converter support lying on the extensive group breach supremacy circuitry strategy be projected primary, the topological arrangement of supremacy electronic grip transformer be specified. next, the scheme organize policy counting spill H-bridge solo- stage rectifier, double lively H-bridge converter manage, inverter grip glide vector organize, plus support converter productivity electrical energy manage be agreed. associated investigate resolve offer a hard base within the growth of extensive group fissure supremacy plans plus the elevated electrical energy huge capability tool functions.

**Keywords**—railing consignment electrical constrain; extensive group fissure; circuitry machinery; elevated supremacy motor

## 1. Introduction

measure up to by conservative si support supremacy circuitry procedure, the original extensive group fissure supremacy partially conductor diplomacy contain individuality of extensive group fissure, elevated serious EF power, elevated diffusion velocity, plus elevated diffusivity, which be able to arrive at superior endure electrical energy standards plus earlier button velocity, inferior change thrashing, and [1-6]advanced working connection warmth than si campaign subsequently, the extensive group fissure supremacy circuitry device can significantly reduce the load, capacity, plus rate of the supremacy electronic converter, advance the effectiveness with supremacy concentration of the supremacy electronic machine , a ~10 &advance the presentation of the supremacy electronic scheme. How in the direction of diminish the load plus quantity of quick prepare grip scheme be individual of the input equipment inside speedy prepare machinery of railing transportation electrical make, plus the solution toward limit the velocity of speedy prepare additional. by the growth of elevated supremacy electronic equipment, multi stage topology plus power equipment, [11-14] supremacy electronic Transation contain conventional additional plus extra concentration. suitable toward the greater individuality of extensive group fissure

supremacy equipment, request determination seriously get better the routine of railing transfer supremacy broadcast motors inside conditions of quantity, burden, plus effectiveness. commencing a capability viewpoint, the newly start on SiC Metal Oxide Semiconductor Field Effect Transistor machine be able to get together the insist intended for RPS inside supplementary motors intended for the railing shipment electrical make. The fast growth of the machine be likely toward be functional inside the major grip force scheme intended for the railing shipment inside the expectations.

The study intends the topology plus manage plan of elevated control support plus grip motors found on top of the extensive group fissure supremacy circuitry equipment future intended for block consignment electrical build since a consequence distinguish the effectiveness advantage lighting load of the quick direct clench create system, which be cooperative to the growth of the seize create system to important speed advantage important superiority. intellectual learning, arithmetical imitation, bonus examination result be accessible to show the power of the designed procedure.

**2. Proposed Work :**

LAYOUT OF MOTOR TOPOLOGY:

PETT exist a unique seize restrain scheme, which be able to decrease the power expenditure plus load via return the usual grip motor of great quantity, important heaviness, plus short effectiveness. on there, the extensively employ PETT topology have a solo stage CHB engine plus DAB motors by average or elevated freq engines. The grip m o t o r component give supremacy intended for the inverter grip motor. A 3-stage AC power resource by modifiable electrical energy amplitude, freq, plus stage be able to be full to 4 similar linked grip motors support on top of a grip inverter. The supplementary motor component give power intended for supplementary tools such since the prepare supporter plus the illumination light. by stage DC electrical energy, 4 flow H-bridge component inside sequence be desirable on slightest via 1.7kV IGBTs otherwise Sic MOSFET machine intended for supplementary motors component.

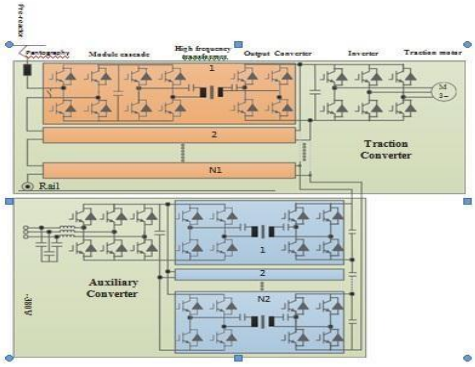


[15~18]

Fig. 1. the topological structure of PETT

I. approaching methodology

*A. CH-bridge Solo-stage Rectifier*

The Fig.2. $U_s$ , $U_{d1}$, $U_{d2}$,…$U_{dN}$ *are used for* dc bus voltage of all CH-bridge $U_{dc}$ is the sum of CHB dc motor vehicle voltage, $i_s$ is position of network effort I, $U_{dc}^*$ position of dc motor vehicle electrical energy, $U_{ad}$ rectifier IP electrical energy. The manage plan comprise electrical energy external round, I internal circle plus C electrical energy adaptive power. The interruption of network voltage be able to be remove during the electrical energy supply advance return.

*B. D A H-bridge motor power*

The supremacy equilibrium be in charge of plan intended for all unit plus double stage transfer PWM be accept which be able to attain the V, I plus supremacy allocation manage of all component. via minimizing the DAH-bridge scheme stricture, such since the feature impedance, the relation of button freq plus ringing freq plus electrical energy change proportion, the backflow supremacy ofmotor be condensed considerably more than a extensive weight collection.

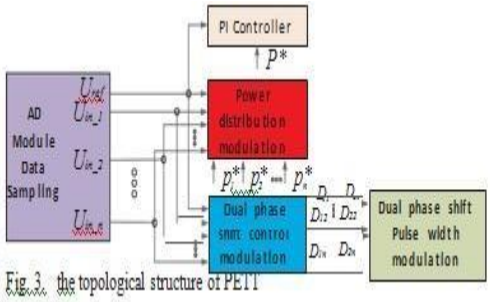


Fig. 3. the topological structure of PETT

*C. M o t o r grip Vector manage*

The Fig.4 comprise the instability plan component by the effectiveness minimization, the d-axis electrical energy supply frontward, the q- axis electrical energy supply frontward, rotor instability viewer unit plus PWM.

*D. secondary motor productivity electrical energy manage*

The direct plan of secondary motor productivity, which accept the inductor I responseplus V / I supply frontward power. It is attain the immediate path of productivity plus the attainable active path of Voutput below abrupt weight plus abrupt weight circumstances.

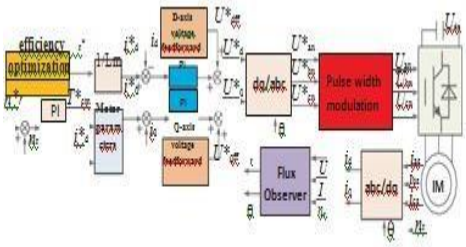


Fig.4. the control strategy of inverter traction motor vector control

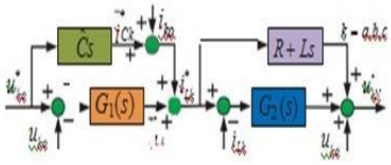


Fig.5. the control strategy of auxiliary converter

I. Replication inside classify toward authenticate the efficiency of the route topology plus the possibility of the manage plan, the reproduction computation plus trial be calculated.

*A. CH-bridge Solo-stage Rectifier*

The scheme exercise 6.5kV IGBTs, group of CH-bridge N1 =12, & the freq is 4 kHz via the yielding button expertise. as of the reproduction consequences, PF=1 process & DC motor vehicle electrical energy manage be attained.

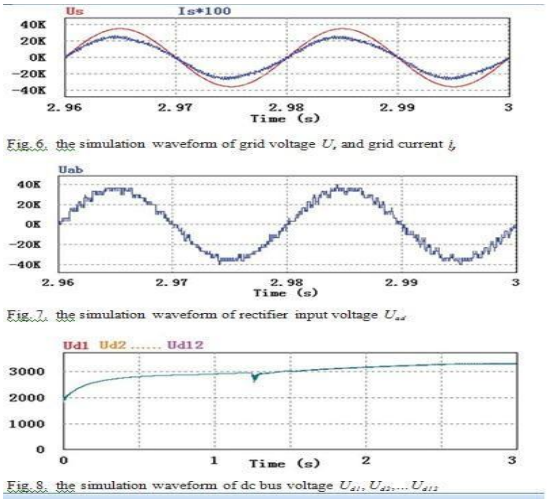


Fig.6. the simulation waveform of grid voltage $U_s$ and grid current $i_s$

Fig.7. the simulation waveform of rectifier input voltage $U_{ab}$

Fig.8. the simulation waveform of dc bus voltage $U_{d1}, U_{d2}, \ldots U_{d12}$

*A. DAH-bridge motor manage*

Fig.10 imitation WF of main twisting electrical energy plus I which have attain the yielding button ringing manage

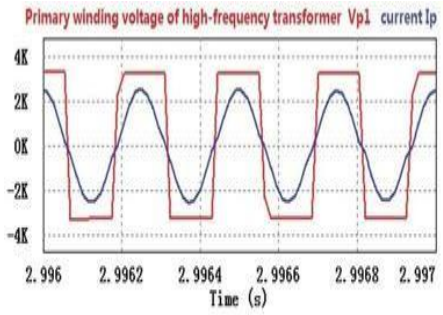


Fig.10 the simulation waveform of primary winding voltage and current of the high frequency transformer

*A. Inverter grip Motor Vector manage:*

As of the replication consequences, the congested ring way result of the grip motor current is superior.

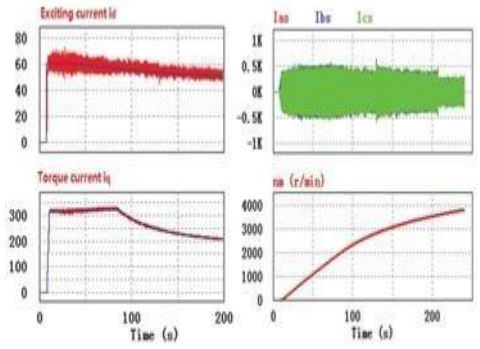


Fig.11. the simulation waveform of exciting current id, torque current iq, traction motor speed nm, three phase current Ias Ibs Ics

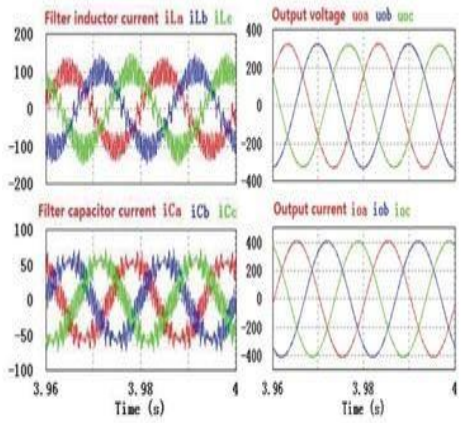


Fig.12. the simulation waveform of exciting current id, torque current iq, traction motor speed nm, three phase current Ias Ibs Ics

Test The CAS300M17BM2 which the speed electrical energy 1200V & 300A. The elevated freq m o t o r accept nano crystalline mixture which the motor revolve 1:1, the pour out inductance is 15 μH. The button freq 43 kHz plus the DC op electrical energy 500V.


Fig. 13. the prototype of dual active H-bridge

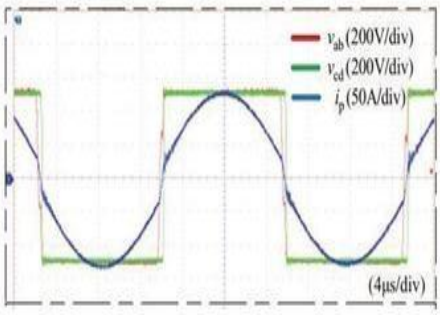


Fig. 14. the experimental waveform of primary winding voltage and current of the high frequency transformer

## II. Conclusion

The PF=1 process plus the DC motor vehicle electrical energy organize of flow H-bridge solo-stage rectifier, the flexible button ringing manage of double vigorous H-bridge motor manage, motor grip speed vector manage plus supplementary motor productivity electrical energy organize be attained.

**References:**

[1] McNutt T, Hefner A, Mantooth H, et al. Silicon carbide power MOSFET model and parameter extraction sequence[J]. IEEE Transactions on Power Electronics,2007,22(2) :353-363.

[2] Kadavelugu A, Baliga V, Bhattacharya S, et al. Zerovoltage switching performance of 1 200V SiC MOSFET,1200V silicon IGBT and 900V CoolMOS MOSFET[C]. 2011 IEEE Energy Conversion Congress andExposition, 2011:1819-1826.

[3] Zhao B, Song Q, Liu W. Experimental comparison of isolated bidirectional DC-DC converters based on all-Si and -SiC power devices for next-generation power conversion application [J]. IEEE Transactions on Indus-trial Electronics, 2014, 61(3):1389-1393.

[4] B Zhao, Q Song, W Liu, Y Sun. Characterization and application of next-generation SiC power devices forhigh-frequency isolated bidirectional DC-DC converter[C]. in Proc. 38th Industrial Electronics Society Con-ference, 2012: 280-285.

[5] Arun Kadavelugu, Seunghun Baek, Sumit Dutta. High-frequency design considerations of dual active bridge 1 200VSiC MOSFET DC-DC converter[C]. In Proc. 26th IEEE the Applied Power Electronics Conference & Exposition, 2011: 314-320.

[6] Y Wang, S W H Haan, J A Ferreira. Potential of improving PWM converter power density with advanced components[C]. In Proceedings of 13th European Conference on Power Electronics and Applications, 2009: 1-10.

[7] Potbhare S, Goldsman N, Lelis A, et al. A physical model of high temperature 4H-SiC MOSFETs[J]. IEEE Transactions on Electron Devices ,2008 ,55(8):2029-2040.

[8] Berning D W, Duong T H, Ortiz-Rodriguez J M, et al. High-voltage isolated gate drive circuit for 10kV,100ASiC MOSFET/JBS power modules[C]. Industry Applications Society Annual Meeting

Edmonton, Canada:IEEE,2008:1-7.

[9] Rabkowski J, Tolstoy G, Peftitsis D, et al. Low-loss high-performance base-drive unit for SiC BJTs[J]. IEEE Transactions on Power Electronics ,2012,27(5):2633-2643.

[10] Wang J, Zhao T, Li J, et al. Characterization,modeling and applicationof 10 kV SiC MOSFET[J]. IEEE Transaction on Electron Devices,2008, 55(8):1798-1805.

[11] Thomas Besselmann, Akos Mester, Drazen Dujic. Power electronic traction transformer: efficiency improvements under light-load conditions[J]. IEEE Transaction on Power Electronics,2014, 29(8):3971-3981.

[12] Jianqiang Liu, Jingxi Yang, Jiepin Zhang, et al. Voltage balance control based on dual active bridge DC/DC converters in a power electronic traction transformer [J]. IEEE Transaction on Power Electronics,2018, 33(2):1696-1714.

[13] Jianqiang Liu, Nan Zhao. Improved fault-tolerant method and control strategy based on reverse charging for the power electronic traction transformer[J]. IEEE Transaction on Industrial Electronics, 2018, 65(3):2672-2682.

[14] Chuanhong Zhao, Drazen Dujic, Akos Mester, et al. Power electronic traction transformer—medium voltage prototype[J]. IEEE Transaction on Industrial Electronics, 2014, 61(7):3257-3268.

[15] Jonas E, Julian Böhler, Daniel Rothmund. Analysis and cell-level experimental verifcation of a 25 kW all-SiC isolated front end 6.6 kV/400 V AC-DC solid-state transformer[J]. IEEE Transaction on Power Electronics and Applications,2017, 2(2):140-148.

[16] Nicolas Hugo, Philippe Stefanutti, Marc Pellerin, Alper Akdag. Power Electronics Traction Transformer[J], European Conference on Power Electronics and Applications, pp.1-10,2007.

[17] C. Zhao, S. Lewdeni-Schmid, J. Steinke, M. Weiss, and M. Pellerin. Design, implementation and performance of a modular power electronic transformer (PET) for railway application,in Proc. 14th Eur. Conf. Power Electron. Appl., Birmingham, U.K., 2011, pp. 1–10.

[18] D. Dujic, C. Zhao, A. Mester, J. Steinke, M. Weiss, S. Lewdeni- Schmid,T. Chaudhuri, and P.Stefanutti,—Power electronic traction transformer—Low voltage prototype[J]. IEEE Trans. Power Electron., vol. 28, no. 12,pp. 5522–5534, Dec. 2013.

[19] 1.Bolla MadhusudanaReddy,Pasala Gopi1,Y.V.Siva Reddy, “Performance improvement of closed loop optimal cascaded high level multilevel inverter fed induction motor drive using ANFIS with low THD and effective speed-torque control” Journal of Electrical Systems, Vol.18, Issue 1, PP.65-81, March 2022.

[20] 2. S.L.V Sravan Kumar. N. Ravi Shankar Reddy,M. Vijay Kumar “Quasi Switched Capacitor based Integrated Boost Series Parallel Fly-Back Converter for Energy Storage Applications” Journal of scientific and industrial research, Vol.78, pp.711-715, July 2019

[21] 3. S.Sarada, N.Ravi sankara Reddy, C.Ganesh, “Reduction of Common Mode Voltage for 3-level Inverter fed DTC of Open End Winding Induction Motor Drive” Test Engineering and Management, Vol.82, Page No. 8754 – 6345 January-February 2020

[22] 4. S. Nithya Lavanya, T. Bramhananda Reddy, M. Vijay Kumar “Vector Control of Induction Motor with Variable Sampling Frequency Random PWM Techniques for Reduced Harmonic Distortion” Test Engineering and Management, Volume 82,Page No. 14688 – 14694,January - February 2020

[23] 5.S.Sarada, Dr.N.Ravi sankara Reddy, “A scalar based SVPWM and DPWM techniques for 3-level inverter fed DTC of open end winding induction motor drive” Jour of Adv research in Dynamical & Control Systems, Volume-10, Issue-13, pp.2553-2568, Sep. 2018.

Materials Today: Proceedings xxx (xxxx) xxx

Contents lists available at ScienceDirect

Materials Today: Proceedings

journal homepage: www.elsevier.com/locate/matpr

# Experimental chatter process stability using end milling process on Al6061 alloy with multiple bearing span conditions

C. Trivikrama Raju [a], S. Jakeer Hussain [b,⇑], G. Yedukondalu [c]

[a] Dept. of Mechanical Engineering, KLEF University, Vaddeswaram, Guntur, India
[b] Dept. of Mechanical Engineering, Mother Teresa Institute of Science and Technology, Sathupally, India
[c] Dept. of Mechanical Engineering, KLEF University, Vaddeswaram, Guntur, India

ARTICLE INFO

*Article history:*
Available online xxxx

*Keywords:*
CNC Milling
Spindle tool structure
Optical Microscope images
Design variables
Al6061Alloy, and bearing span (BS)

ABSTRACT

An end milling process's chatter stability analysis is complicated due to a lack of exact information of the spindle's geometrical design, the location of the bearings, and other spindle structural concerns. Self-excited chatter vibrations can only be studied with an exact transfer function in the most flexible area of the spindle tool structure, which an efficient spindle needs design. A new approach for assessing spindle vibration responses using sine sweep tests for a CNC end milling machine tool is the topic of this research. When the bearing span is considered as a design variable, the spindle's analytical model may be approximated. There are several trial runs until the model and experiment transfer functions agree. To obtain the process stability, the time varying forces are evaluated at the different cutting conditions.

Selection and peer-review under responsibility of the scientific committee of the International Conference on Materials Innovation and Sustainable Manufacturing.

## 1. Introduction

A wide range of industries, including aerospace, automotive, mould and die, and more, still rely on vertical CNC milling forhigh-speed machining. It is possible to improve process efficiency via optimization, but machine tool chatter is the most important factor in the process's efficacy. Uncertainty in the cutting process produces excessive material removal, low surface area, and nearly guaranteed tool and workpiece damage. An accurate dynamic model of the tool-holder-spindle assembly is needed to choose the elements that minimize chatter and improve surface smoothness. In order to get this dynamic at the tool tip, modal testing may be used, but it requires a large number of tool-holder configurations in a production plant. In the case of micro-end mills, the measurements are time-consuming and sometimes troublesome. Analytical and experimental research on spindle modeling utilizing modal test data have been described in a limited number of papers. An end mill's self-excited vibrations may be inversely studied to determine the transfer function (TF), according to a study by Suzuki et al. [1] developed a transfer function to minimize the percentage of error between the numerical and experimental simulations. To account for the rotor dynamic effects, Gagnol et al. [2] employed a new finite element modeling technique for the novelistic spindle bearing system to characterize the spindle's modal variations. In order to verify the models' correctness, they were first tested. Spindle rotational precision may be quantitatively simulated by Kim et al. [3] using statistical models and software. With increasing the spindle's speed, the spindle's rotational precision might vary dramatically. In addition, bearing preload has a significant influence on performance. To determine the spindle unit's speed-varying dynamics and the accompanying stability lobes, Cao et al. [4] used an alternative technique. In high-speed milling processes, the Nyquist stability criterion is used to assess the stability of the milling dynamics. Finite element modeling including the thermal characteristics for the components of the integrated spindle tool system is provided by Zahedi and Movahhedy [5].Six-degree-of-freedom Timoshenko beam components were applied to the spindle housing and shaft. When designing a flat end mill geometry, Flutes may be thought of as helicoidal surfaces, and a flute's shank can be considered a rotating surface in three dimensions, according to Tandon and Khan [6]. Finite-element modeling of milling spindle lateral vibrations and the corresponding displacements are measured and it can be used to analyze these vibrations, according to Rantatalo et al. [7] and Sarhan and Matsubara [8] employed different sensors at various locations on

⇑ Corresponding author.
*E-mail address:* jakeershaik786@gmail.com (S. Jakeer Hussain).

https://doi.org/10.1016/j.matpr.2023.02.341

Selection and peer-review under responsibility of the scientific committee of the International Conference on Materials Innovation and Sustainable Manufacturing.

the spindle tool to obtain the displacements and the corresponding stiffness in the radial direction in order to accurately monitor cutting forces during end milling. Kolar et al.[9] investigated the cutting dynamics of the whole machine tool spindle system, including the machine tool frame. The attached model shows how the spindle and tool system's dynamic characteristics alter in proportion to the machine frame's attributes. For industrial engineers, Cao et al. [10] have updated the FE model so that it can better predict the dynamic response of the spindle tool system. Operating mode analysis was advocated by Zaghbani and Songmene [11] to improve modal characteristics and correct performance metric estimates in various machining scenarios. This was followed by an experiment wherein we used the dynamic process parameters to draw stability lobes. Zivkovic et al. [12] presented a thermo mechanical spindle model and it was relied on the ball bearing contact bearings. Temperature affects the stiffness of a spindle in a non-linear way, and this is tested and validated. Various numerical improvements in the simulation, machining mistakes in curved surfaces, tool indentation effects and vibrations created in inclined and circular surfaces have all been studied extensively. Preload influence on spindle and tool tip frequency responses was presented by Ozturk [13]. An explanation of the spindle's preload-to-spindle-speed relationship was given. Spindle unit modal analysis was performed in the no-run situation in all of the preceding studies. Accordingly, the dynamic modal parameters of the cutting process will change as a result of the different cutting circumstances. The modal properties of machining at different process parameters are estimated in this study. Spindle bearings on the front and back of the spindle unit are evaluated in the study of the complete spindle unit. There are two ways to estimate the modal parameters: first, using Timoshenko beam theory and second, using shear deformation effects. The dynamic state modal parameters are discovered via a series of experiments. Other parts were ordered as follows: (2) Spindle assembly modeling (3) Results and discussion and then (4) Conclusions.

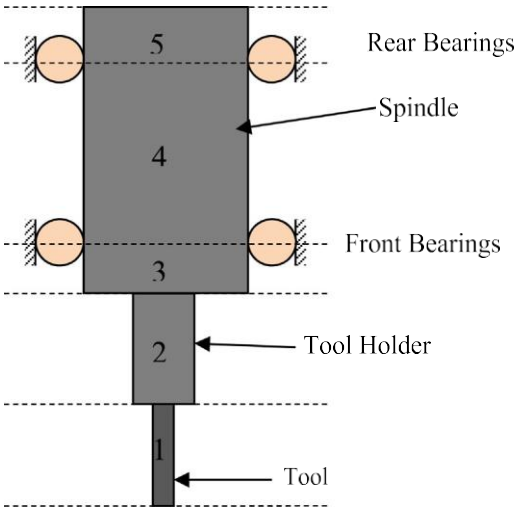


Fig. 1. Finite element beam model of the spindle tool unit.

## 2. Modeling of spindle assembly

High-precision applications need accurate tool dynamics identification. Input forces and output responses are often measured using experimental modal analysis. However, it can only be used if the machine tool is not in use at the time of application. During a cutting operation, the worktable sliding locations affect the tool structure's dynamics. Previous studies have indicated that the machine tool's structural dynamics change as a function of the tool's location or spindle speed. Many experiments are carried out due to this. For this reason, data collected during a static condition differs from that collected during a cutting process. The calculation of dynamic spindle structural characteristics with work table cutting motion on spindle dynamics is one of the research's outstanding questions. It is possible to accurately measure the spindle tool response with the angular contact bearings with proper constrained system as indicated in the Fig. 1. Timoshenko beam components with shear deformation and rotational inertia effects are used to descrtized all the sections of the integrated spindle tool unit.

In the present analysis, two bending deflections in y and z and one linear deflection (i.e.,x direction) are included in the total of 24 degrees of freedom for the overall spindle unit. Two angular contact bearings are assumed to support the spindle unit's two nodes. Fig. 2 shows the position of the entire spindle tool system with the spring connections as well as the bearing connections.

Also, as with the spindle shaft, the tool holder is attached to the tool. The following is a description of the unit's finite element model:

$$[M_b]\{\ddot{q}\} + [C_b] - \Omega[G_b]]\{\dot{q}\} + [K_b] - \Omega^2[M_{cb}]\{q\} = F(t) \quad (1)$$

Here, $[M_b]$, $[K_b]$ and $q[M_{cb}]$ are the combined mass, viscous damping, and stiffness $[K_b]$ matrixes for the beam element, is the rotation speed, while $[G_b]$ represents the gyroscopic matrix and the term $2[M_{cb}]q$ denotes the softening impact of spring forces. There are a number of factors that affect angular contact bearings' stiffness. Bearings with radial stiffness (Static Radial Stiffness) may be assessed using several empirical equations, such as the ball diameter ($D_b$), the axial preload ($F_a$), the contact angle of static angular-contact ball bearing, and the number of balls ($N_b$).

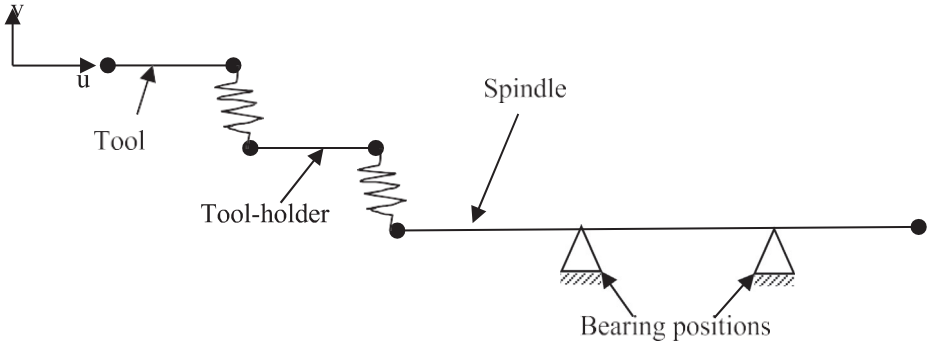


Fig. 2. Line model of the spindle-tool unit with spring and bearing connections.

$$k_{xx} = k_{yy} = 1.77236 \times 10^{7} \times N_b^{2} \cdot D_b^{1=3} \frac{\cos^2 h}{\sin^{1=3} h} F_a^{1=3} \; N=m \qquad (2)$$

*Cutting dynamics*

Using a well-known mechanical model for milling, chatter is generated by the cutting force. Fig. 3 shows various instances of milling cutters by considering a two degree of freedom model with a zero helix angle and $N_t$ is the number of teeth. The work piece is treated as the rigid in nature and the cutting tool is considered as the flexible in nature. Vibration is caused by the whole amount of cutting power.

The radial (n) thickness of the chip is used to represent the variable chip thickness

$$h(u_j) = f_t \sin(u_j)(n_{j-1} - n_j \; g(u_j) \qquad (3)$$

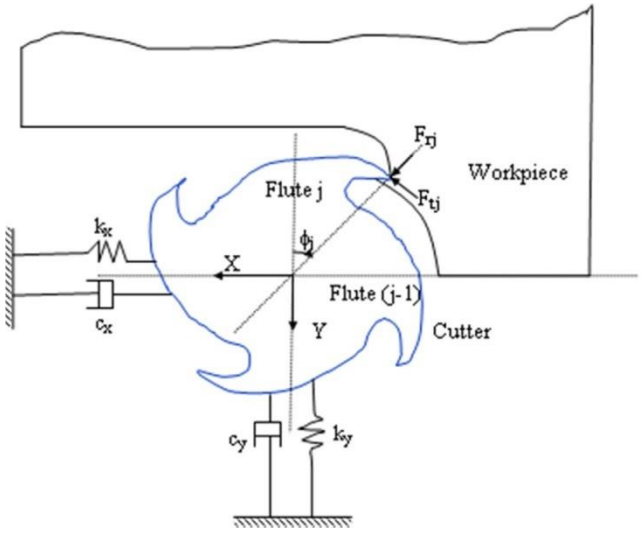


Fig. 3. Two-degree of freedom milling model.

The Eigen value equation for chatter frequency $x_c$, static cutting factors ($K_t$, $K_r$), radial immersion angles ($u_s$ and $u_e$) and the frequency response function of the structure are worked out using the formula. By means of,

$$j = \frac{K_{Im}}{K_{Re}} = \frac{\sin x_c s}{1 - \cos x_c s} \qquad (4)$$

The analytical stability limit for the predicted frequency responses are arrived as follows:

$$b_{\lim} = -\frac{2p}{N_t K_t} K_{Re}(1 + j^2) \qquad (5)$$

The following tooth passages have a phase change of$e = p - 2w$. Next, the tooth passing times are stated as$s = \frac{1}{x_c}(e + j2p)$, here j represents integer and is the lobe number for each tooth. All that's left to do is plot the stability lobe between the spindle speeds and the graph.

$$X = \frac{60}{N} s(rpm) \qquad (6)$$

## 3. Results and discussions

The experimental modal analysis is verified using a full-order finite element technique. For this experiment, the settings listed in Table 1. were employed.

The stability barrier is tested using a CNC milling machine with the same spindle. These machines are equipped with three-axis motion with spindles that can spin at up to 4,000 rpm. A HSS end mill cutter cutting tool with four edges and with a diameter of 12 mm fits into the tool holder. Aluminum alloys are milled completely. Fig. 4 shows the list of components for predicting the vibration response using an accelerometer with a charge amplifier and oscilloscope.

While the transmission's amplitude stays constant, the frequency of the signal is modulated. At each input frequency level, the oscilloscope captures corresponding accelerometer responses from the vibration shaker on the cutting tool. It is possible to see

Table 1
Parameters of the full-order finite element model.

| Parameter | Element of the spindle E1 E2 E3 E4 E5 | | | | |
|---|---|---|---|---|---|
| Length(mm) | 65 | 51 | 111 | 90 | 47 |
| diameter(mm) | 12 | 40 | 75 | 75 | 75 |
| E (Pa) | $2.35 \times 10^{11}$ | $2.1 \times 10^{11}$ | $2.1 \times 10^{11}$ | $2.1 \times 10^{11}$ | $2.1 \times 10^{11}$ |


Fig. 4. Experimental set-up employed.

the responses' amplitudes for each frequency in Fig. 5. Natural frequencies in this range are 1910 Hz and 2550 Hz, as you can see.

Stability lobe diagrams based on analytical predictions are used to perform experiments at different speeds and depths of cut. Charge amplifier and acclerometer are linked to the non-rotating section of the spindle to measure the cutting tool's vibration response during milling. Using an optical microscope with a magnification factor of 10X is used to acquire the images of the machining areas. Fig. 6 shows the chatter marks on the workpiece material with a cutting speed of 2200 rpm and a depth of cut is taken as 0.07 mm. The machining reaches the chatter prone zones as indicated in Fig. 6, if cutting surpasses the limit of 0.07 mm as indicated in Fig. 6(b).

The oscilloscope is used to capture the vibrations of the cutting tool in the time domain. Figs. 7 and 8 illustrate the amplitudes and FFT graphs for axial depths of 0.07 mm and 0.09 mm, respectively. Increasing the axail depth of cut results in an increase in tool vibration, which causes chatter marks on the workpiece as a result of this vibration.

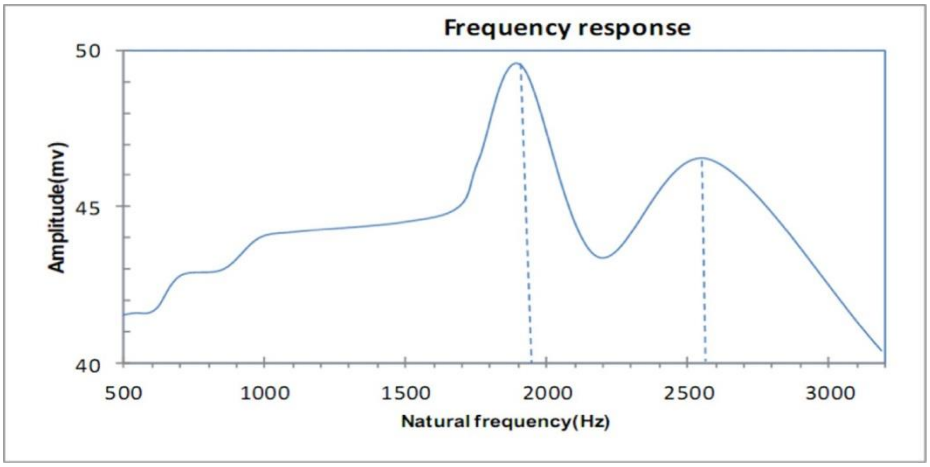


Fig. 5. Tool tip frequency response of the spindle-tool unit.

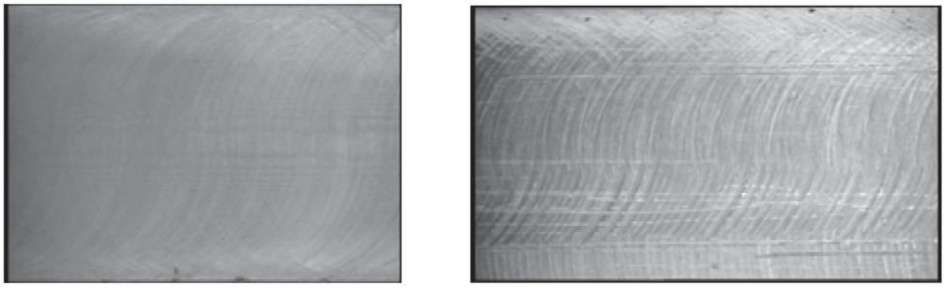

(a) Axial depth of cut 0.07mm (b) Axial depth of cut 0.09mm

Fig. 6. Optical microscopic images of machining areas.

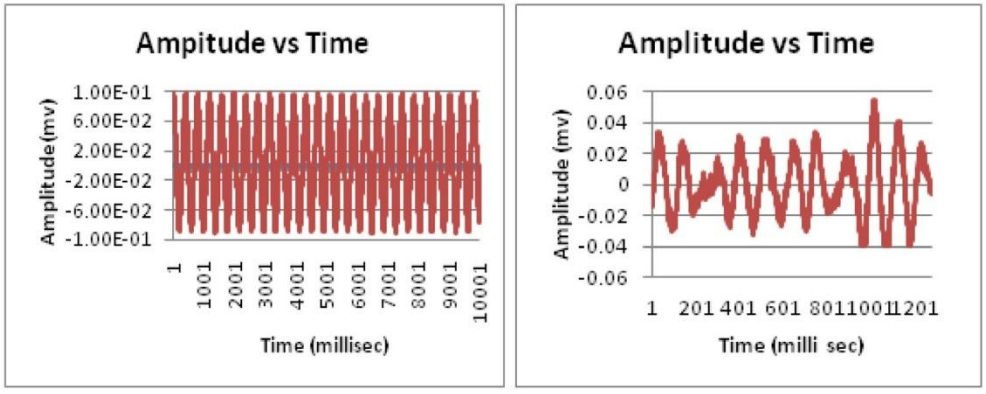


(a) Axial depth of cut 0.07mm (b) Axial depth of cut 0.09mm

Fig. 7. Tool vibrations at different depths of cut.

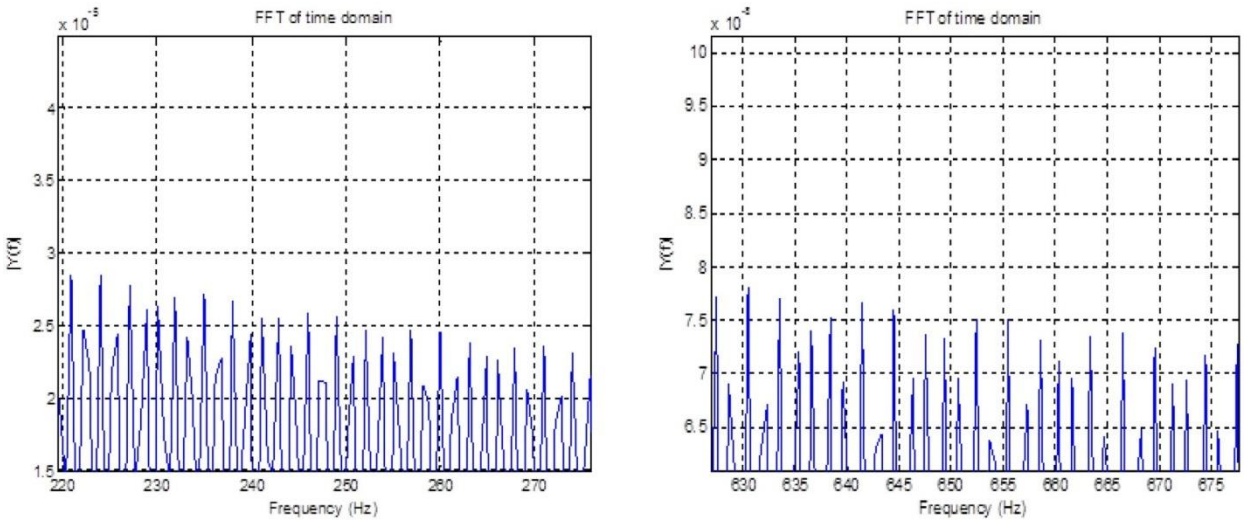


(a) Axial depth of cut 0.07mm (b) Axial depth of cut 0.09mm

Fig. 8. FFT plots at different depths of cut.

Analytical stability lobe diagrams are interpolated by considering the tool vibration levels and optical microscopic images of the machining areas. Fig. 9 shows that the theoretically anticipated lobes are giving correct bounds for experimental results.

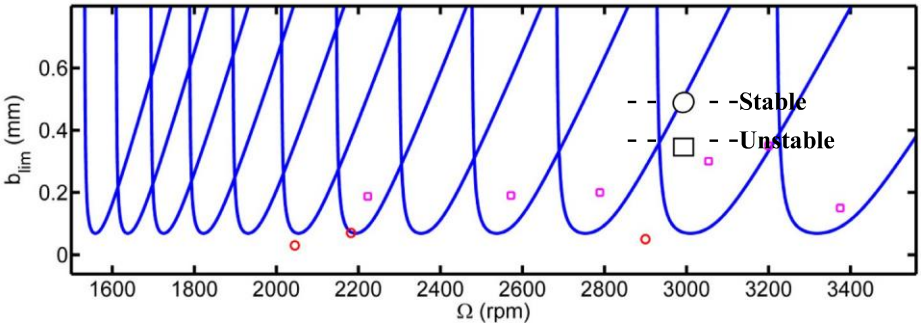


Fig. 9. Analytically predicted stabilty lobes at different depths of cut.

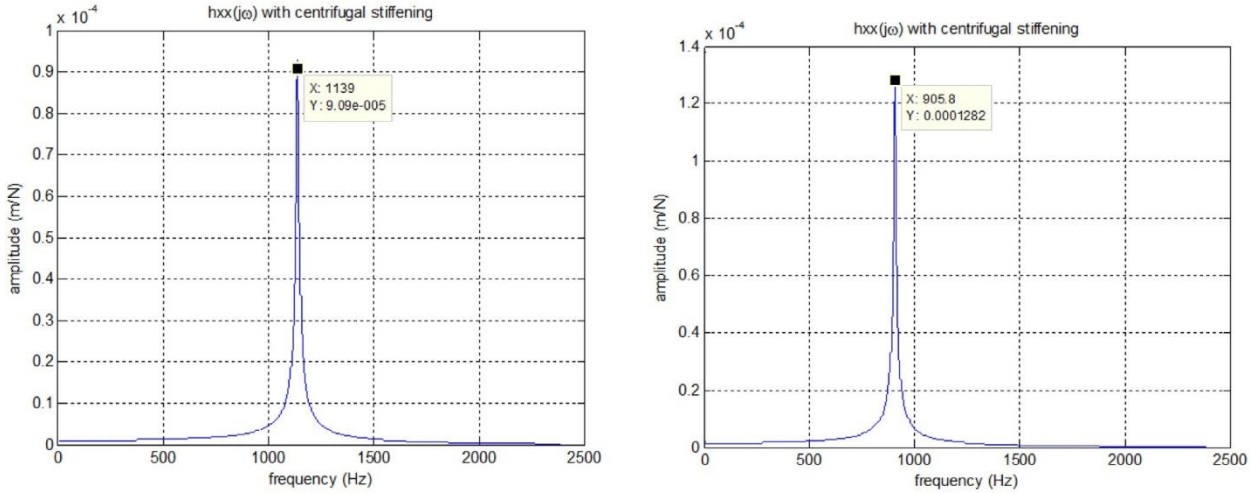


(a) Tool overhang of 85mm (b) Tool overhang of 95mm

Fig. 10. Frequency responses at two overhang lenghts.

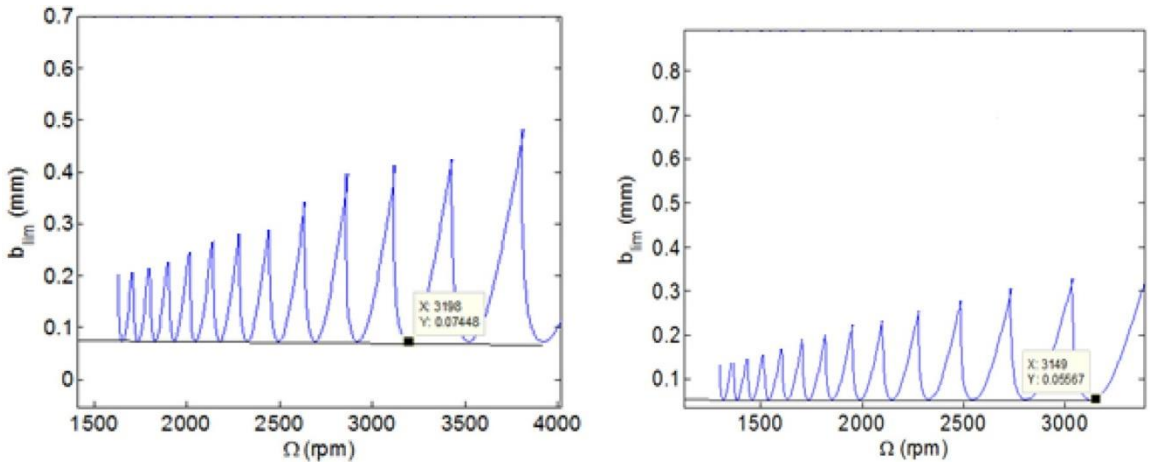


(a) Tool overhang of 85mm (b) Tool overhang of 95mm

Fig. 11. Stability plots at two different overhang lenghts.

When it comes to determining milling instability, the average axial depth of cut and the dynamic stiffness play a key role in the design of machining process. Many key design factors are associated with these problems, including the size of the spindle shaft and the positions of its housing and bearings, as well as bearing preload, tool overhang, and the cutting tool's helix angle. The stability of slot milling for varying tool overhang lengths is examined in this study. As shown in Fig. 10, tool overhang length has a significant impact on system stability. When the cutting tool's overhang length increases, the peak first mode of the natural frequencies shifts to the left side of the amplitude axis.

It is observed that, when the tool overhang length increases there is slight decrement in the average stable depth of cut and it is indicated in the Fig. 11. When examining the spindle dynamic system's natural frequency in the first mode has affected the overhang length of the tool and also has the greatest impact on the system's milling dynamics.

## 4. Conclusions

Finite element analysis employing Timoshenko beam theory with rotational and shear deformation effects was used to examine a real spindle tool unit in the current study. On the CNC milling centre, a spindle device-tool holder experimental modal analysis is performed to arrive at the tool tip FRF. Trail runs using tool overhang as the design parameter may be used to estimate the modal since isolating the spindle from the housing is difficult. Nonlinear bearing forces as well as cutting forces were taken into account at certain nodes while determining the spindle tool unit's dynamic stability. Both the cutting tests and the numerical simulations, which used the identical applied circumstances, yielded later similar FFT displays.

## Data availability

Data will be made available on request.

## Declaration of Competing Interest

The authors declare that they have no known competing financial interests or personal relationships that could have appeared to influence the work reported in this paper.

## Acknowledgement

The author(s) declare that there is no conflict of interest regarding the publication of this paper. The author(s) also declare that they have no known competing financial interests or personal relationships that could have appeared to influence the work reported in this paper

## References

[1] N. Suzuki, Y. Kurata, T. Kato, R. Hino, E. Shamoto, Identification of transfer function by inverse analysis of self-excited chatter vibration in milling operations, Precis. Eng. 36 (2012) 568–575.
[2] V. Gagnol, T. PhuLe, P. Ray, Modal identification of spindle-tool unit in high-speed machining, Mech. Syst. Sig. Process. 25 (2011) 2388–2398.
[3] J.D. Kim, I. Zverv, K.B. Lee, Model of rotation accuracy of high-speed spindles on ball bearings, J. Sci. Res. 2 (2010) 477–484.
[4] H. Cao, B. Li, Z. He, Chatter stability of milling with speed-varying dynamics of spindles, Int. J. Machine Tools & Manuf. 52 (2012) 50–58.
[5] A. Zahedi, M.R. Movahhedy, Thermo-mechanical modeling of high-speed spindles, Scientia. Iranica. B. 19 (2) (2012) 282–293.
[6] P. Tandon, M.D. Rajik Khan, Three-dimensional modeling and finite element simulation of a generic end mill, Comput.-Aided Design 41 (2009) 106–114.
[7] M. Rantataloa, J.O. Aidanpaab, B. Goranssonc, P. Normand, Milling machine spindle analysis using FEM and non-contact spindle excitation and response measurement, Int. J. Machine Tools & Manuf. 47 (2007) 1034–1045.
[8] A.D. Ahmed Sarhan, A. Matsubara, Investigation about the characterization of machine tool spindle stiffness for intelligent CNC end milling, Robotics and Comput.-Integrated Manuf. 34 (2015) 133–139.
[9] P. Kolar, J.M. Sulitka, Simulation of dynamic properties of a spindle and tool system coupled with a machine tool frame, Int. J. Adv. Manuf. Technol. 54 (2011) 11–20.
[10] H. Cao, B. Li, Z. He, Finite element model updating of machine-tool spindle systems, J. Vib. Acoustics 135 (2013) 0245031–0245034.
[11] I. Zaghbani, V. Songmene, Estimation of machine-tool dynamic parameters during machining operation through operational modal analysis, Int. J. Machine Tools & Manuf. 49 (2009) 947–957.
[12] A. Zivkovic, M. Zeljkovic, S. Tabakovic, Z. Milojevic, Mathematical modeling and experimental testing of high-speed spindle behavior, Int. J. Adv. Manuf. Technol. 77 (2015) 1071–1086.
[13] E. Ozturk, U. Kumar, S. Turner, T. Schmitz, Investigation of spindle bearing preload on dynamics and stability limit in milling, Int. J. Machine Tools & Manf 61 (2012) 343–346.

Materials Today: Proceedings xxx (xxxx) xxx

Contents lists available at ScienceDirect

Materials Today: Proceedings

journal homepage: www.elsevier.com/locate/matpr

# Investigation of the cutting-edge radius size effect on dynamic forces in micro end milling of brass260

C. Trivikrama Raju [a], S. Jakeer Hussain [b,⇑], G. Yedukondalu [c], Ahmed M. Galal [d,e]

[a] Dept. of Mechanical Engineering, KLEF University, Vaddeswaram, Guntur, India
[b] Dept. of Mechanical Engineering, Mother Teresa Institute of Science and Technology, Sathupally, India
[c] Dept. of Mechanical Engineering, KLEF University, Vaddeswaram, Guntur, India
[d] Production Engineering and Mechanical Design Department, Faculty of Engineering, Mansoura University, P.O 35516, Mansoura, Egypt
[e] Department of Mechanical Engineering, College of Engineering in Wadi Alddawasir, Prince Sattam bin Abdulaziz University, Saudi Arabia

ARTICLE INFO

*Article history:*
Available online xxxx

*Keywords:*
Tool-tip dynamics
Micro-end milling
Cutting force coefficients
Uncut chip thickness
Tool edge radius
Brass 260 Alloy

ABSTRACT

Rapid increases in the number of industries that need a sub-micron surface finish on 3D micro/meso technological innovation parts are being seen. Due to the high rotating speeds of activities, chatter behaviour also occurs during micro-cutting. Changes in bearing stiffness, gyroscopic effects, and misalignment are only some of the factors that need to be considered while studying the spindle's dynamics. By regulating the movement of the cutting edge, the cutting action may be made more consistent. The structure of the tools also affects the machine's dynamics. Since the modes of different machine-tool components interact with one another, the dynamics of the tool tip are affected. In this research, we consider a model of a micro spindle system to enhance machining accuracy. Timoshenko beam theory is used to account for shear deformation and rotational inertia effects due to the short and thick beam-type designs of each component of the micro tool. A detailed dynamical model of the moving micro end mill is created using an extended form of Hamilton's Principle. A two-degree-of-freedom model of the micro-milling process considers the modal dynamic properties of the tool-holder-spindle assembly and the micro-milling cutting forces. A three-dimensional finite element model of the system is built, and its dynamic response is gathered, to validate the full order finite element approach. Cutting force coefficients are then modelled as a function of instantaneous uncut chip thickness, which is principally affected by the tool edge radius and feed per tooth at different radial immersion depths.

Selection and peer-review under responsibility of the scientific committee of the International Conference on Materials Innovation and Sustainable Manufacturing.

## 1. Introduction

In the industrial industry, where every second counts, high-speed machining (HSM) is gaining ground. This is necessary because many industries (such as aircraft, biomedicine, medical devices, and communications) demand ever-increasing levels of accuracy and miniaturization. Improvements in micro milling have made it common practice to produce mechanical and other components with fine details in a broad variety of materials. The capacity to construct intricate 3D geometries, a high material removal rate, a relatively smooth surface, and a wide variety of machinable materials are just a few of the many ways in which this method excels above other micromanufacturing techniques. Although material removal in micro milling relies on mechanical contact between the tool cutting edges and the workpiece material, this interaction also leads to tool deflections, tool wear, and tool breakage, which are all problems in a manufacturing context. Practically, many size effects develop and the whole material removal geometry changes when the size of the tool and the material removal unit are reduced in comparison to standard size cutting operations. Cutting forces in micro milling are notoriously difficult to forecast since the feed per tooth is so much bigger in relation to the cutter radius. Also, unlike regular milling, micro milling is significantly impacted by run-out of the tool tip, which may occur even at the micrometer scale. To avoid early wear and breakage of the micro-mill flute and to obtain the smooth surface finish and needed precision on the smallest components, special considera- tion must be given to the tool geometry, cutting speed, chip load,

* Corresponding author.
*E-mail address:* jakeershaik786@gmail.com (S. Jakeer Hussain).

https://doi.org/10.1016/j.matpr.2023.02.339
2214-7853/
Selection and peer-review under responsibility of the scientific committee of the International Conference on Materials Innovation and Sustainable Manufacturing.

and depth of cut. Cutting forces may be considered of as the "fingerprint" of a process since they are intimately correlated with process parameters, the average cutting-edge radius, and the integrity and wear of the tool. As a result, cutting forces may be used in a variety of contexts, including but not limited to: parameter selection; part accuracy estimate; tool wear monitoring; process stability assessment. However, micro milling cutting force measurement is complicated, requiring specialized expertise and high-priced equipment. Cutting force, stress, temperature, and vibration may be predicted using knowledge of the different properties of workpiece material, different tool conditions and various cutting process parameter conditions. Modeling the cutting mechanics and dynamics may allow for prediction of the process behavior during micro-milling. Many writers have developed methods for dynamically modelling micro end mills. The analytical mathematical cutting force model of the integrated micro end milling dynamics was investigated by Filiz and Ozdoganlar, and it took into account factors such as setup errors, axial force, sectioned tool geometry, and the actual cross section of the twisted fluted section. [1]. Bissacco et al. [2] developed a numerical model for the prediction of the cutting force model and its influence on the over the cutting radius size effect, deviation of the tip of the cutting tool and its chip flow angle along with the inclination angle and tool run out effect. Huang et al. [3] evaluated the use of maximum vibration amplitude to determine cutting forces in micro milling and compared their results to those of other studies. Ding et al. [4] formulated a three-dimensional model for cutting forces to shed light on the cutting forces experienced during 2D vibration-assisted micro end-milling. Mustapha and Zhong [5] developed a new hybrid analytical cutting force model to estimate the transverse cutting forces in a micro end mill. The model was discretized into structural components so that damping and stiffness coefficients of the machining system could be taken into account. Shi et al. [6] investigated the impacts of gyroscopic and mode-interaction effects on the dynamics and stability of a micro end-mill during regeneration chatter. During cutting operations, the micro-end mill's transfer behavior was monitored utilizing piezoelectric components. Using the goal of better comprehending the dynamic characteristics of a micro end mill, Huang et al. [3] investigated a novel dynamic cutting force model for a micro stepped end mill with the time dependent cutting boundary conditions. Dynamic qualities were considered, and factors including rotational velocity, cutting depth, and boundary stiffness were considered. Jin and Altintas [7] examined the use of cutting force coefficients derived from FE model assessments to the problem of predicting micro-milling forces. In addition to this strain hardening and its strain rate along with temperature effects are considered for the analysis. The predicted cutting forces were used to develop mechanical models, with model force coefficients taken as the nonlinear functions of the uncut chip thickness and its tool edge radius effects. The calculated cutting forces in different directions seen in experiments were compared to those anticipated by the FE and the slip-line field models previously developed. When the radius of the cutting tool is enhanced there is a raise in the cutting forces increases, but the other parameters like effectiveness of stress and average temperature at the cutting zone decrease dramatically, as shown by Yang et al. [8]. When working with a micro-cutter, it was found that the radius of the tool's cutting edge had the largest influence on how hot the cutting edges were. The new micro-spindle designed by Jahanmir et al z. [9] and Li et al. [10] can reach speeds of up to 500,000 rpm, making it ideal for micro-milling. The experimental results demonstrated that the micro-dynamic spindle was stable by analyzing the vibration spectra collected during free rotation and cutting. Despite the accessibility of information on the micro milling dynamics of the forces and its mechanism of formation etc. and also there is a need for further study to overcome various barriers in actually performing these operations, with a micro end mill being the key focus.

A finite element model of a micro end-milling process with a coupled spindle and tool is presented in the present investigation. The vibration response of the micro end-mill system is studied. Timoshenko beam theory is used to determine the governing equations for the micro end-mill, which is modelled as a stepped distributed dynamic system. This spindle system is analyzed in the same way, using a three-dimensional finite element model to represent the system as a solid. Modal and harmonic analyses confirm the arriving of the dynamic modes of frequency of the integrated spindle tool unit. A theoretical model is investigated for micro end-milling cutting force prediction, considering the influence of cutting-edge radius size.

## 2. Mathematical Modeling

Micro end mill spindle system schematic shown at a high level in Fig. 1. (Capable of speeds between 10,000 and 60,000 rpm). The spindle shaft is built with a hollow circular cross section with an upward taper at its front to house the cutting tool holder at its position. This integrated portion of the tool holder and collet can be approximated with taper section along with the spindle is considered to be with the uniform portion. Similarly, the micro end-mill tool's shank radius should correspond to the tool holder's inner radius (including the collet). The micro-end mill used in this illustration has the dimensions shown in Fig. 2: a tool diameter of 0.6 mm, a shank diameter of 4 mm, and an overhang of 16 mm from the tool holder. Micro end mills' free shank lengths are typically rather short, hence shear deformation may be accounted for by using Timoshenko beam theory. Slopes in two bending directions are shown in this case, where and are bending and shear angular deflections, respectively. Each beam elements are considered with a total of four degrees of freedom per node and are used for the discretization of the micro end-mill tool (i.e. at each node point with two translatory motions along with the two rotations). These sorts of displacements are disregarded since the milling system is so rigid in the axial and torsional axes.

To represent a rotating beam, we use a finite beam element with gyroscopic effects, based on the Timoshenko beam theory developed by Nelson [11]. Applying Hamilton's concept yields the mass matrices for translation and rotation of an element, as well as its stiffness matrix and gyroscopic matrix. The FE approach yields the following matrix form for the governing equation:

$$[M]\{\ddot{q}\} + [C]\{\dot{q}\} + [K] - \Omega^2[M_c]\ \{q\} = F \qquad (1)$$

where [G] is the gyroscopic matrix, [M] is the mass matrix, [C] is the viscous damping matrix, and [K] is the stiffness matrix, where $\Omega$ is the rotational speed, and the phrase $\Omega^2[M_c]\{q\}$ denotes the dampening effect of spring forces. Without a time-integration method, the real and imaginary components of the FRF may be written as follows:

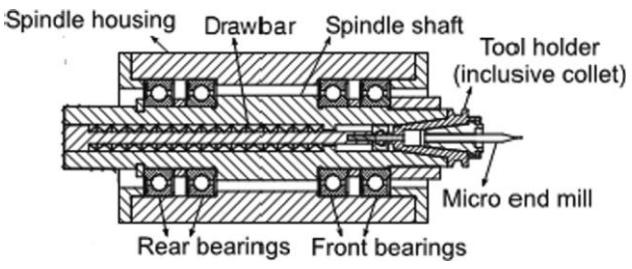


Fig. 1. Micro end-mill spindle unit diagram.

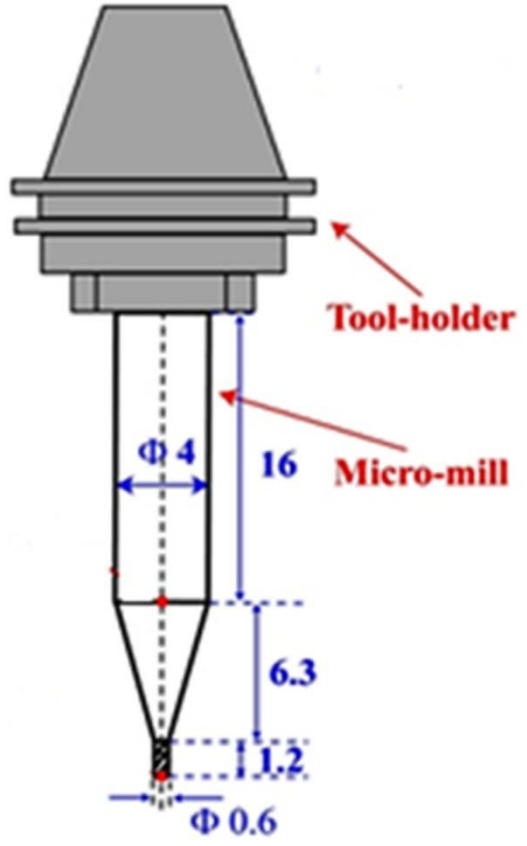


Fig. 2. Model for equivalent analysis.

$$[H(j\omega)] = [Re(\omega)] + j[Im(\omega)] = [I] - \omega^2[M][K] + j\omega[C]^{-1} \quad (2)$$

The real and imaginary components of the spindle tool tip transfer function are denoted by Re and Im, respectively. ANSYS 13 uses a 3D finite element approach to forecast the micro-inherent mill's frequencies and mode shapes. At the tip of the shank, a perfect cantilever restriction is imposed. The spindle system is meshed using solid 187 components in a three-dimensional solid model of a micro end-mill. Carbide was chosen as the material for the micro end-mill system, with the density and elastic modulus assumed to be 14300 kg/m³ and 580 GPa, respectively. Cylinders with diameters equal to 90% of the marginal value of the tip diameter serve as approximations for all the flutes of the cutting tool.

## 3. Numerical micro end milling cutting force model

Cutting force study plays a very crucial role to understand the mechanics and dynamics of the machining process. Not having optimal cutting conditions may lead to tool breakage, which in turn costs time and money. Tool wear and fractures are also difficult to see for the operator. Cutting force analysis is therefore crucial in micro-end-milling for establishing cutting plans and establishing cutting conditions, as well as for determining cutting process features such as tool wear and surface roughness. The following tangential and normal (feed) cutting force components may be predicted using a slip-line field model:

$$F_t = K_t(h; r)hw$$
$$F_n = K_n(h; r)hw \quad (3)$$

The width of the cut, w, is equal to the total of the differential depth of cut, D, where h is the uncut chip thickness. After that, you may get the initial cutting force coefficients with varying chip thickness(h) of the uncut portion with a nonlinear curve fitting method to numerically simulated the cutting forces and is shown below.

$$K_t(h; r) = a_t{:}h^{pt} + b_t{:}h^{qt}r^{st}$$
$$K_n(h; r) = a_n{:}h^{pn} + b_n{:}h^{qn}r^{sn} \quad (4)$$

The evaluation of the cutting forces with different effects like chip thickness(t) ratio and tool-edge radius(r) are considered with the empirical constants (p, q, and s). When the radius of tool being used for the cutting is same as the chip being removed from the workpiece is drastically rises nonlinearly. removed during cutting, nonlinearity rises. Cutting forces are seldom impacted by the cutting speed, which may be anywhere between 19 and 45 m per minute. Thus, in the current model, the coefficients are considered to be unrelated to the cutting speed. The relevant information for this instance is shown in Table 1.

Here we have an expression for chip thickness vs feed per tooth (f) and its tool angular position (/)for a time-dependent tool:

$$h(\phi) = f\sin(\phi) + v(t) - v(t - T_p) \quad (5)$$

$$v(t) = x(t)\sin(\phi) + y(t)\cos(\phi)$$

Li et al. provide a simplified form of the equation (5). For example, to express [10] in terms of the radius of the tool being used, we have

$$h(\phi) = r\left(1 - \sqrt{1 - \frac{2f\sin(\phi)}{r} + \frac{f^2\cos(2\phi)}{r^2} + \left(\frac{2\pi}{N_f}\right)\cos\phi + \left(\frac{2\pi}{N_f}\right)^2}\right) + f\sin(\phi)\cos(\phi)\left(\frac{2\pi}{N_f}\right) + \frac{1}{2}\left(\frac{2\pi}{N_f}\right)^2\cos(\phi) \quad (6)$$

Here assuming, the variable axial depth of cut(a), by considering the tangential and normal cutting forces with uncut chip thickness for any cutting edge can be taken as follows:

$$dF_t = K_t h(\phi)da$$
$$dF_n = K_n h(\phi)da \quad (7)$$

The instantaneous cutting force coefficients Kt and Kn and / is the immediate angular location of the tooth edge. Considering the effect of the helix angle over the differential angular location, the

Table 1
Empirical cutting force coefficients of the brass260 alloy.

| constants | a | b | p | q | s |
|---|---|---|---|---|---|
| $K_t$ | 914.4 | 62.61 | −0.0004 | −0.814 | 0.2302 |
| $K_n$ | 629.9 | 78.24 | −0.0002 | −0.786 | 0.2469 |

Table 2
Parameters for the micro end-mill spindle for the FEM analysis.

| Parameter | Elements of the spindle | | | | | |
|---|---|---|---|---|---|---|
| | 1 | 2 | 3 | 4 | 5 | 6(Holder) |
| Length (mm) | 1.2 | 2.1 | 2.1 | 2.1 | 16 | 20 |
| Outer dia.(mm) | 0.6 | 0.8 | 1.2 | 2.5 | 4 | 8 |
| Inner dia. (mm) | 0 | 0 | 0 | 0 | 0 | 0 |
| E (Gpa) | 580 | 580 | 580 | 580 | 580 | 580 |

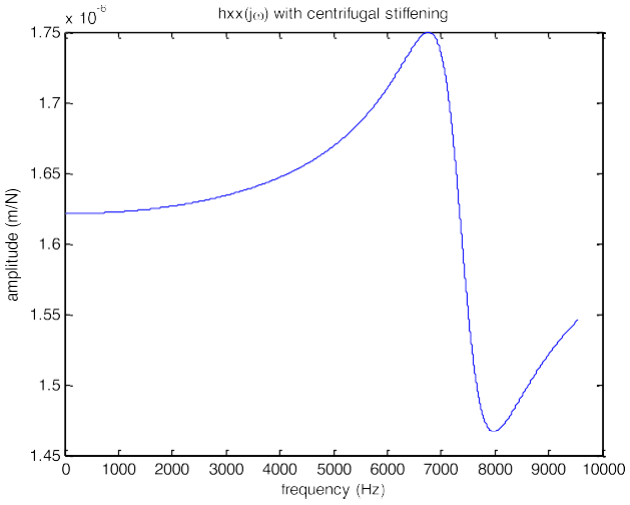


Fig. 3. Frequency response at tool tip for 36000 rpm.

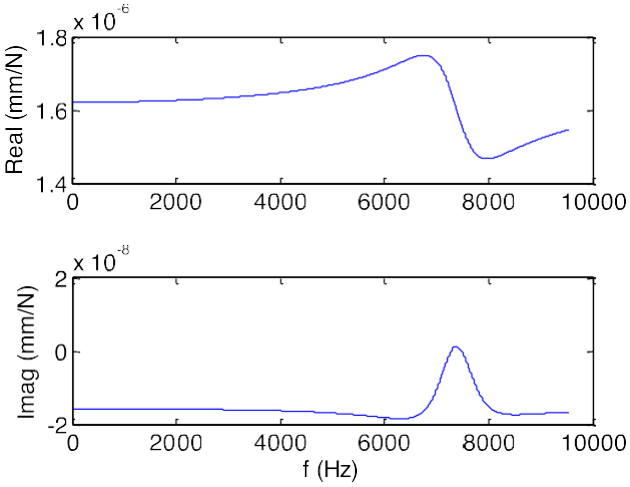


Fig. 4. Both real and imaginary FRF at 36,000 rpm.

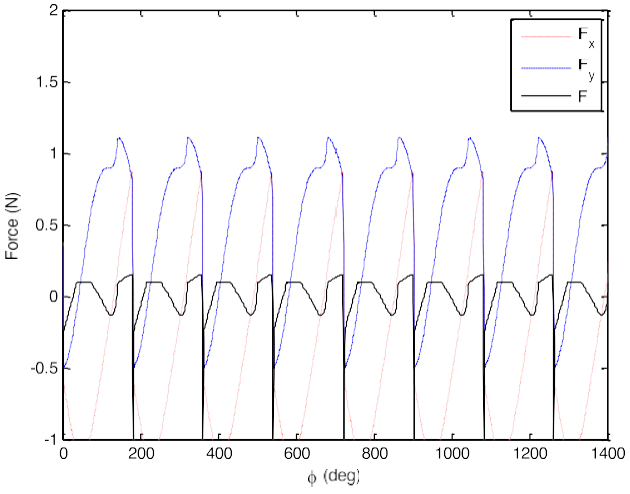


Fig. 5. Numerical cutting forces at O = 36 k rpm, feed = 1 lm/tooth, depth of cut = 50 lm, tool edge radius = 8 lm.

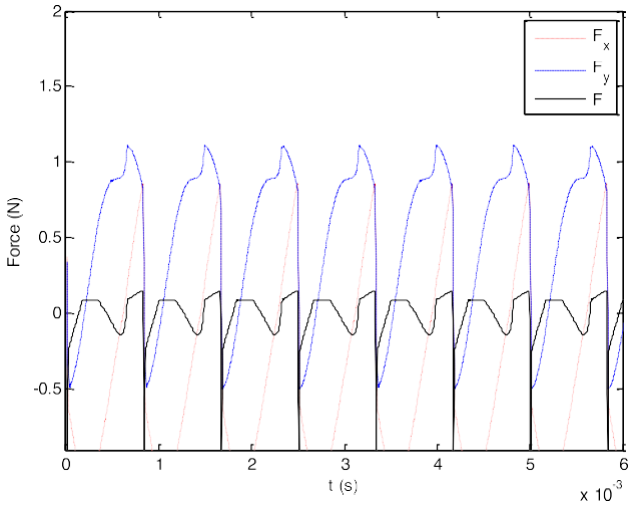


Fig. 6. Numerical cutting forces at O = 36 k rpm, feed = 1 lm/tooth, depth of cut = 50 lm, tool edge radius = 8 lm.

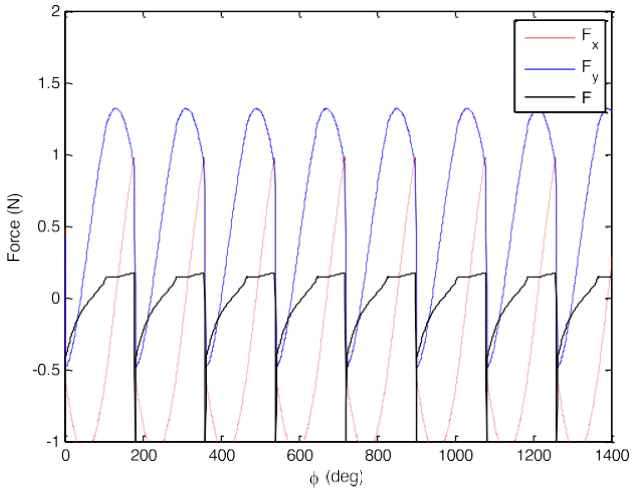


Fig. 7. Numerical cutting forces at O = 36 k rpm, feed = 1 lm/tooth, depth of cut = 50 lm, tool edge radius = 10 lm.

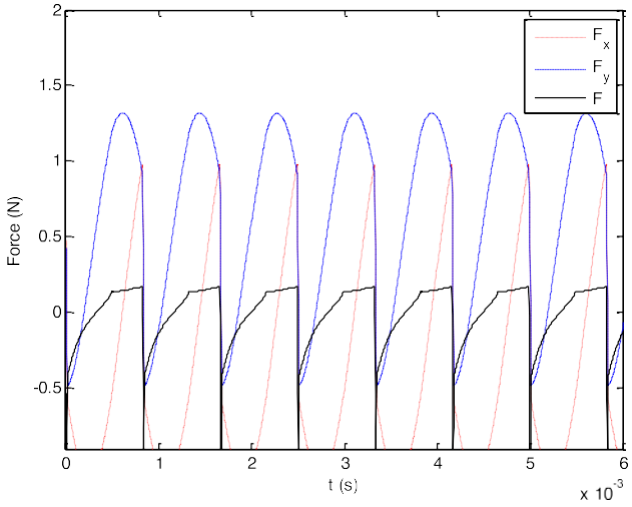


Fig. 8. Numerical cutting forces at O = 36 k rpm, feed = 1 lm/tooth, depth of cut = 50 lm, tool edge radius = 10 lm.

corresponding forces are zeros when / is not in the cutting zone between entry ($/_s$) and exit angles ($/_e$) of the cutter at each axial step. Assuming a free end of the mill feed, the cutting forces exerted are

$$dF_x(u) = -dF_t\cos(u) - dF_n\sin(u)$$
$$dF_y(u) = dF_t\sin(u) - dF_n\cos(u) \quad (8)$$

The cutting forces imparted by the N flute of the cutting tool in conjunction with the axial depth of the cut to estimate the overall milling forces as follows:

$$F_x(u) = \sum_{i=1}^{N}\int_0^a dF_x\, u\,(i-1)\frac{2p}{N}\,du \quad (9a)$$

$$F_y(u) = \sum_{i=1}^{N}\int_0^a dF_y\, u\,(i-1)\frac{2p}{N}\,du \quad (9b)$$

## 4. Results and discussions

The micro end-mill is a six-element tool, the first of which is attached to the mill body (end). The idealised beams have three stages, with the last two being the shank and the holder, to account for the tapering section. Table 2 shows the values used in the spindle finite element model.

To examine the integrated micro end mill spindle mechanism, a computer programme is written in MATLAB. The software includes

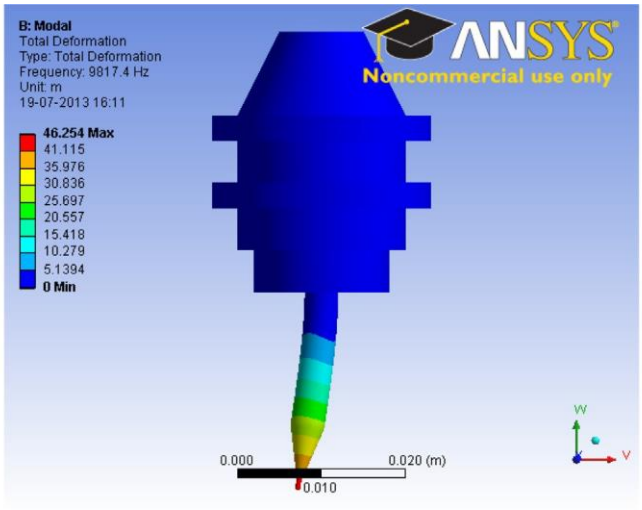


(a) First mode

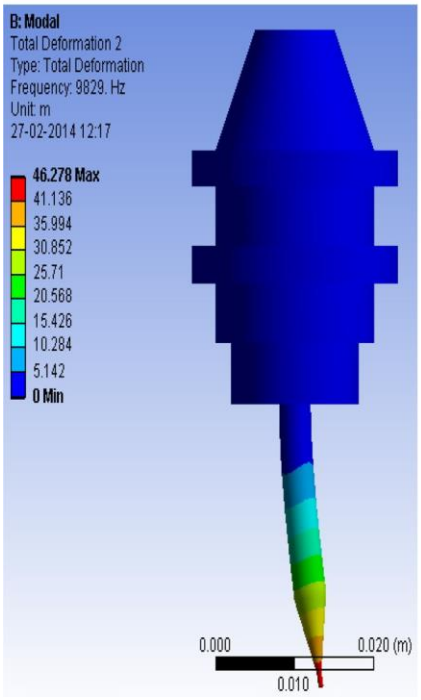


(b) Second mode

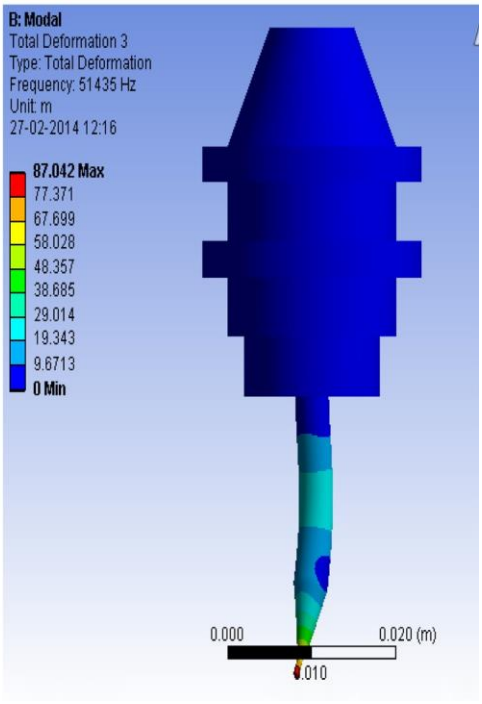


(c) Third mode

Fig. 9. Modes of deformation of the shank portion and tool tip.

assembly matrices and a static condensation method for removing rotational degrees of freedom, both of which make the initial assumption that positions for the bearing were assumed to be rigid. The tool tip frequency response is shown in Fig. 3. Considering the solid damping for the whole system, Fig. 4 shows the corresponding real and imaginary plots for the tool unit system at frequencies between 8000 Hz and 9000 Hz.

However, unlike traditional end milling, micro end milling utilises a much larger feed per tooth to tool radius ratio. Therefore, it is crucial to properly adjust the specific conditions of the cutting process. The basic parametric study for the mechanistic traditional milling modelling processes have already been undertaken by a number of writers in their previous publications. This paper presents a novel technique for deriving cutting force coefficients from numerical simulation output that takes into consideration the ploughing effect in micro machining. Each coefficient is written as a non-linear function of the current chip thickness. The provided framework allows for time domain cutting force prediction on the basis of cutting force coefficients and different cutting situations. The simulation is programmed in MATLAB, and the results are shown visually in Figs. 5–8. Also taken into account is complete immersion slot milling, in which the radial depth of cut is equal to the cutter's diameter. The following quantitative parameters are used in the current work: Specifications: feed rate (f) = 1–2 m /tooth, axial depth of cut (a) = 50 m, spindle speed = 36 krpm, and tool radius (r) = 30 m.

When the value of the cutting tool edge radius is enhanced from 8 m to 10 m, the cutting force shifts from 1.06 N to 1.36 N, as shown in the Simulated Cutting forces. The process parameters such as feed per tooth, spindle speed and axial depth of cut were

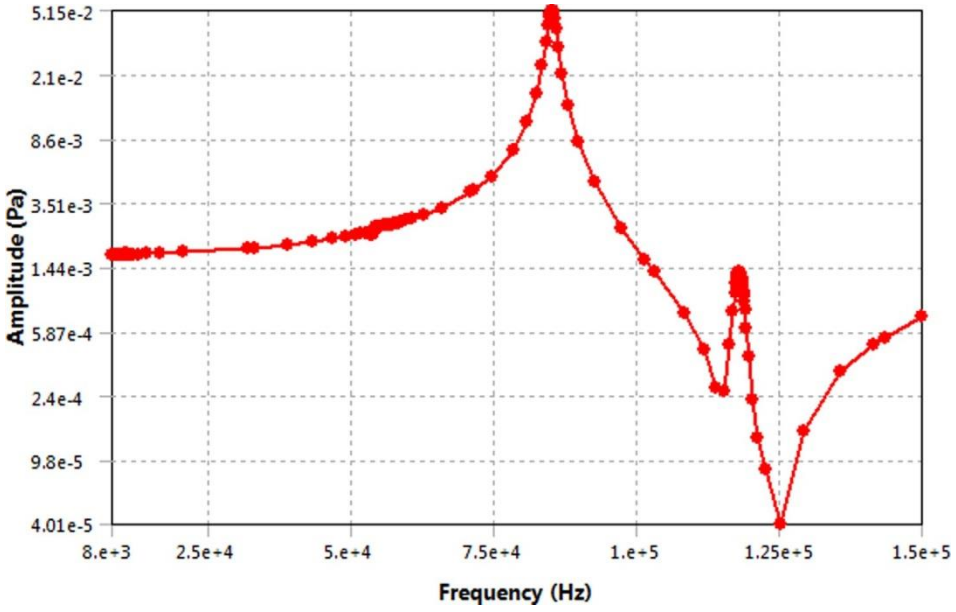


Fig. 10. Harmonic response of the system.

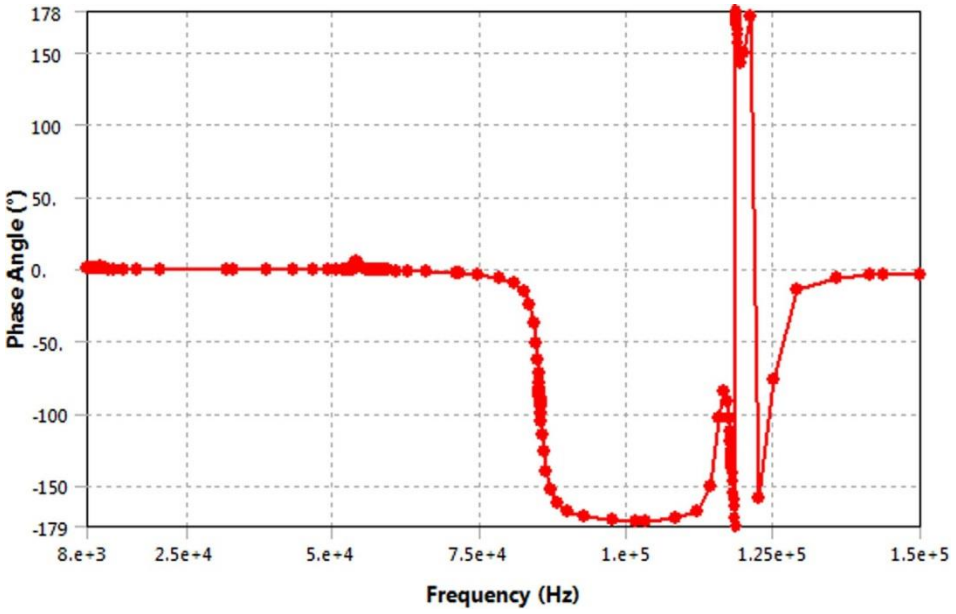


Fig. 11. Response of Phase for the micro-end mill.

held constant. Cutting forces required to dampen the tool's self-excited vibrations are very sensitive to the radius of the cutting edge (r). Fig. 9(a), 9(b), and 9(c) show the resonant frequencies and mode forms of the first, second, and third bending modes, respectively (c). Z-axis is the undeformed axial direction of the tool. The primary mode of vibration is derived from taper end portion of the tool holder and bending of the tip of the tool, as shown by the finite element analysis. The boundary condition at the clamping point of the tool causes modification in tool dynamics, as shown by the discrepancy in natural frequencies between validation from the beam theory and the finite element prediction.

The first four modes of the micro end mill spindle system are analysed by modal analysis, and the resulting frequencies are 9817.4 Hz, 9829 Hz, 51435 Hz, and 51493 Hz. To assess the dynamic behaviour of the micro end-mill spindle tool system the harmonic response analysis is performed, the results of which may be seen in Fig. 10 as the peak responses on a graph of displacements against frequencies. The natural frequencies have been proven accurate by the mode superposition technique. In order to assess how much a response lags after the applied load, we have displayed the phase response alongside the harmonic plots, as shown in Fig. 11.

## 5. Conclusions

In the present paper, the entire spindle tool unit is analyzed by utilizing the Timoshenko beam theory with the shear deformation, rotational and along with the centrifugal effects. The dynamic spindle model is used to derive frequency response functions for the working at the tip of the tool. The end mill tool of micro milling model's FRF is compatible with both analytical and numerical models, allowing for precise stability lobe diagrams to be built for high-velocity milling. During the second stage, a three-dimensional finite element analysis is used to get a dynamic response from the system's solid model. Predicting cutting forces on a micro scale is crucial for making informed choices about cutting factors, designing effective miniature tools, and assessing the feasibility of machining requirements. Cutting force simulations show that raising the feed rate results in a rising pattern of cutting force. In order to properly build the cutting tool one that can sustain vibrations during cutting without wearing out this tool edge radius is a crucial geometric element.

## Data availability

Data will be made available on request.

## Declaration of Competing Interest

The authors declare that they have no known competing financial interests or personal relationships that could have appeared to influence the work reported in this paper.

## Acknowledgement

The author(s) declare that there is no conflict of interest regarding the publication of this paper. The author(s) also declare that they have no known competing financial interests or personal relationships that could have appeared to influence the work reported in this paper

## References

[1] S. Filiz, O.B. Ozdoganlar, Micro endmill dynamics including the actual fluted geometry and setup errors-Partl: model development and numerical solution, J. Manuf. Sci. Eng. 130 (2008) 1–10.
[2] G. Bissacco, H.N. Hansen, J. Slunsky, Modelling the cutting-edge radius size effect for force prediction in micro milling, CIRP Annals-Manuf. Technol. 57 (2008) 113–116.
[3] B.W. Huang, J.Z. Cai, W.L. Hsiao, Cutting force estimation in a micro milling process, J. Eng. Manuf. 224 (2010) 1615–1619.
[4] H. Ding, S.J. Chen, K. Cheng, Two-dimensional vibration-assisted micro end milling: cutting force modelling and machining process dynamics, J. Eng. Manuf. 224 (2010) 1775–1783.
[5] K.B. Mustapha, Z.W. Zhong, A hybrid analytical model for the transverse vibration response of a micro-end mill, J. Mech. Syst. Signal Process. 34 (2013) 321–339.
[6] Y. Shi, F. Mahr, U. Wagner, E. Uhlmann, Gyroscopic and mode interaction effects on micro-end mill dynamics and chatter stability, Int. J. Adv. Manuf. Technol. 65 (2013) 895–907.
[7] X. Jin, Y. Altintas, Prediction of micro-milling forces with finite element method, J. Mater. Process. Technol. 212 (2012) 542–552.
[8] K. Yang, Y. Liang, K. Zheng, Q. Bai, W. Chen, Tool edge radius effect on cutting temperature in micro-end-milling process, Int. J. Adv. Manuf. Technol. 52 (2011) 905–912.
[9] S. Jahanmir, Z. Ren, H. Heshmat, M. Tomaszewski, Design and evaluation of an ultrahigh speed micro-machining spindle, Mach. Sci. Technol. 14 (2014) 224–243.
[10] H.Z. Li, K. Liu, X.P. Li, A new method for determining the undeformed chip thickness in milling, J. Mater. Process. Technol. 113 (2001) 378–384.
[11] H.D. Nelson, A finite rotating shaft element using Timoshenko beam theory, J. Mach. Des. 102 (1980) 793–803.

Elite

# NPTEL Online Certification

(Funded by the MoE, Govt. of India)

This certificate is awarded to

**BALA SWAMY MADANU**

for successfully completing the course

## Principles of Management

with a consolidated score of **62** %

| | | | |
|---|---|---|---|
| Online Assignments | 22.81/25 | Proctored Exam | 39/75 |

Total number of candidates certified in this course: **6619**

**Prof. Sanjeev Manhas**
Coordinator, Continuing Education Centre
IIT Roorkee

**Jan-Apr 2023**
**(12 week course)**

Priti Maheshwari

**Prof. Priti Maheshwari**
NPTEL Coordinator
IIT Roorkee

Indian Institute of Technology Roorkee

FREE ONLINE EDUCATION swayam शिक्षित भारत, उन्नत भारत

Roll No: NPTEL23MG33S64914465

To validate the certificate

No. of credits recommended: 3 or 4

# NPTEL-AICTE
# Faculty Development Programme

(Funded by the MoE, Govt. of India)

*This certificate is awarded to*

**BALA SWAMY MADANU**

*for successfully completing the course*

**Principles of Management**

*with a consolidated score of* **62 %**

Prof. Andrew Thangaraj
NPTEL Coordinator
IIT Madras

**(Jan-Apr 2023)**

Roll No: NPTEL23MG33S64914465

Duration of NPTEL course : 12 Weeks

The candidate has studied the above course through MOOCs mode, has submitted online assignments and passed proctored exams.
This certificate is therefore acceptable for promotions under CAS as per AICTE notifications dated 24th July 2018, similar to other refresher / orientation courses.
**F.No. AICTE / RIFD / FDP through MOOCs / 2017-18**

# NPTEL Online Certification

(Funded by the MoE, Govt. of India)

This certificate is awarded to

**DR M V RAMACHANDRA RAO**

for successfully completing the course

## Quantum Mechanics I

with a consolidated score of **41** %

| | | | |
|---|---|---|---|
| Online Assignments | 10.69/25 | Proctored Exam | 30.75/75 |

Total number of candidates certified in this course: **15**

**Jan-Apr 2023**

**(12 week course)**

**Prof. Sridhar Iyer**
Head CDEEP & NPTEL Coordinator
IIT Bombay

Indian Institute of Technology Bombay

FREE ONLINE EDUCATION swayam शिक्षित भारत, उन्नत भारत

Roll No: NPTEL23PH04S54913857

To validate the certificate

No. of credits recommended: 3 or 4

Elite

# NPTEL Online Certification

(Funded by the MoE, Govt. of India)

This certificate is awarded to

**DR MANJUNATH BE**

for successfully completing the course

## Cloud Computing and Distributed Systems

with a consolidated score of **69** %

| | | | |
|---|---|---|---|
| Online Assignments | 25/25 | Proctored Exam | 43.5/75 |

Total number of candidates certified in this course: **2219**

**Prof. B. V. Ratish Kumar**
Chairman, Centre for Continuing Education
IIT Kanpur

**Jan-Mar 2023**
**(8 week course)**

**Prof. Satyaki Roy**
NPTEL Coordinator
IIT Kanpur

Indian Institute of Technology Kanpur

FREE ONLINE EDUCATION swayam शिक्षित भारत, उन्नत भारत

Roll No: NPTEL23CS27S45860777

To validate the certificate

No. of credits recommended: 2 or 3

Elite

# NPTEL Online Certification

(Funded by the MoE, Govt. of India)

This certificate is awarded to

**G RAVI RAJU**

for successfully completing the course

## Cloud Computing and Distributed Systems

with a consolidated score of **72** %

| | | | |
|---|---|---|---|
| Online Assignments | 25/25 | Proctored Exam | 46.5/75 |

Total number of candidates certified in this course: **2219**

**Prof. B. V. Ratish Kumar**
Chairman, Centre for Continuing Education
IIT Kanpur

**Jan-Mar 2023**

**(8 week course)**

**Prof. Satyaki Roy**
NPTEL Coordinator
IIT Kanpur

Indian Institute of Technology Kanpur

FREE ONLINE EDUCATION swayam शिक्षित भारत, उन्नत भारत

Roll No: NPTEL23CS27S45861145

To validate the certificate

No. of credits recommended: 2 or 3

# NPTEL Online Certification

(Funded by the MoE, Govt. of India)

This certificate is awarded to

**G RAVI RAJU**

for successfully completing the course

## Data Base Management System

with a consolidated score of **45** %

| | | | |
|---|---|---|---|
| Online Assignments | 11.04/25 | Proctored Exam | 33.75/75 |

Total number of candidates certified in this course: **3478**

**Aug-Oct 2022**

**(8 week course)**

**Prof. Debjani Chakraborty**
Coordinator, NPTEL
IIT Kharagpur

Indian Institute of Technology Kharagpur

FREE ONLINE EDUCATION swayam शिक्षित भारत, उन्नत भारत

Roll No: NPTEL22CS91S34160444

To validate the certificate

No. of credits recommended: 2 or 3

# NPTEL-AICTE
## Faculty Development Programme

(Funded by the MoE, Govt. of India)

This certificate is awarded to

**K S R K SUNIL**

for successfully completing the course

**Applied Linear Algebra in AI and ML**

with a consolidated score of **58 %**

Prof. Andrew Thangaraj
NPTEL Coordinator
IIT Madras

**(Jan-Apr 2023)**

Roll No: NPTEL23MA31S64915107

Duration of NPTEL course : 12 Weeks

The candidate has studied the above course through MOOCs mode, has submitted online assignments and passed proctored exams.
This certificate is therefore acceptable for promotions under CAS as per AICTE notifications dated 24th July 2018, similar to other refresher / orientation courses.
**F.No. AICTE / RIFD / FDP through MOOCs / 2017-18**

# NPTEL Online Certification

(Funded by the MoE, Govt. of India)

This certificate is awarded to

**K S R K SUNIL**

for successfully completing the course

## Applied Linear Algebra in AI and ML

with a consolidated score of **58** %

| | | | |
|---|---|---|---|
| Online Assignments | 10.94/25 | Proctored Exam | 47.25/75 |

Total number of candidates certified in this course: **115**

**Jan-Apr 2023**

**(12 week course)**

**Prof. Debjani Chakraborty**
Coordinator, NPTEL
IIT Kharagpur

Indian Institute of Technology Kharagpur

FREE ONLINE EDUCATION swayam शिक्षित भारत, उन्नत भारत

Roll No: NPTEL23MA31S64915107

To validate the certificate

No. of credits recommended: 3 or 4

# NPTEL-AICTE
## Faculty Development Programme

(Funded by the MoE, Govt. of India)

*This certificate is awarded to*

**SHAIK FHYSUDDIN**

*for successfully completing the course*

**Introduction to Embedded System Design**

*with a consolidated score of* **50 %**

Prof. Andrew Thangaraj
NPTEL Coordinator
IIT Madras

**(Jan-Apr 2023)**

Roll No: NPTEL23CS06S34913584

Duration of NPTEL course : 12 Weeks

The candidate has studied the above course through MOOCs mode, has submitted online assignments and passed proctored exams.
This certificate is therefore acceptable for promotions under CAS as per AICTE notifications dated 24th July 2018, similar to other refresher / orientation courses.
**F.No. AICTE / RIFD / FDP through MOOCs / 2017-18**

# NPTEL-AICTE
## Faculty Development Programme

(Funded by the MoE, Govt. of India)

This certificate is awarded to

**MR NANDYALA VINOD KUMAR**

for successfully completing the course

**Air Pollution and Control**

with a consolidated score of **52 %**

Prof. Andrew Thangaraj
NPTEL Coordinator
IIT Madras

**(Jan-Apr 2023)**

Roll No: NPTEL23CE14S54710101

Duration of NPTEL course : 12 Weeks

The candidate has studied the above course through MOOCs mode, has submitted online assignments and passed proctored exams.
This certificate is therefore acceptable for promotions under CAS as per AICTE notifications dated 24th July 2018, similar to other refresher / orientation courses.
**F.No. AICTE / RIFD / FDP through MOOCs / 2017-18**

# NPTEL Online Certification

(Funded by the MoE, Govt. of India)

This certificate is awarded to

**MR NANDYALA VINOD KUMAR**

for successfully completing the course

## Air Pollution and Control

with a consolidated score of **52** %

| | | | |
|---|---|---|---|
| Online Assignments | 17.5/25 | Proctored Exam | 34.5/75 |

Total number of candidates certified in this course: **7382**

**Prof. Sanjeev Manhas**
Coordinator, Continuing Education Centre
IIT Roorkee

**Jan-Apr 2023**
**(12 week course)**

**Prof. Priti Maheshwari**
NPTEL Coordinator
IIT Roorkee

Indian Institute of Technology Roorkee

Roll No: NPTEL23CE14S54710101

To validate the certificate

No. of credits recommended: 3 or 4

# NPTEL Online Certification

(Funded by the MoE, Govt. of India)

This certificate is awarded to

**MR NANDYALA VINOD KUMAR**

for successfully completing the course

## Hydraulic Engineering

with a consolidated score of **51** %

| | | | |
|---|---|---|---|
| Online Assignments | 21.13/25 | Proctored Exam | 30/75 |

Total number of candidates certified in this course: **84**

**Jan-Apr 2023**

**(12 week course)**

**Prof. Debjani Chakraborty**
Coordinator, NPTEL
IIT Kharagpur

Indian Institute of Technology Kharagpur

FREE ONLINE EDUCATION swayam शिक्षित भारत, उन्नत भारत

Roll No: NPTEL23CE35S34710071

To validate the certificate

No. of credits recommended: 3 or 4